ESRF	**Experiment title:** Time-resolved Bragg coherent X-ray diffraction imaging of the kinetics of physical processes in functional materials	**Experiment number**: MA-4441
Beamline: ID01	**Date of experiment**: from: 27 Jan 2021 to: 01 Feb 2021	**Date of report**: 10/09/2021
Shifts: 15	**Local contact(s)**: Edoardo Zatterin	*Received at ESRF:*

Names and affiliations of applicants (* indicates experimentalists):

T.W. Cornelius, S. Labat*, O. Thomas, Aix-Marseille University, CNRS, IM2NP UMR 7334, Marseille, France

J. Eymery, M.-I. Richard, M. Dupraz, CEA/IRIG, Grenoble, France

C. Dubourdieu, Helmholtz Center Berlin, Germany

A. Kholkin, Ural Federal University, Yekaterinburg, Russia

Report:

This proposal was initially a long-term proposal focusing on the development of time-resolved imaging of dynamics of ferroelectric domains by Bragg coherent X-ray diffraction. The LTP was converted into a standard proposal. Due to the COVID-19 pandemic and the restrictions regarding the number of users on site as well as the preparation of samples for BCDI, we decided to perform scanning X-ray diffraction microscopy (SXDM) instead. The aim of this experiment was the imaging of the strain field in the ferroelectric domains and in the vicinity of the domain walls in ferroelectric crystals. Here, we studied periodically polarized $LiNbO_3$ (ppLN), $ErMnO_3$, and HfO thin films.

The incident X-ray beam at ID01 was monochromatized to 8 keV and focused to a size of 70 nm x 70 nm using a Fresnel zone plate made out of gold. Scanning X-ray diffraction microscopy was performed by mapping 10 x 10 µm² areas with a step size corresponding to the beam size at 25 different incident angles at a given Bragg reflection. These measurements were repeated at 3 independent Bragg peaks in order to eventually obtain the full strain tensor.

Figure 1 shows a scanning X-ray diffraction map of a ppLN crystal taken at the (-2 4 -2 12) Bragg peak revealing the periodic domain structure. A complete scanning X-ray diffraction microscopy image was taken of one of the domains by mapping at different incident angles. The deviation $\Delta\mu$ of the three measured Bragg reflections (0 0 0 12; 3 0 -3 12; -2 4 -2 12) from their center-of-mass (COM) along the Q_x, Q_y, and Q_z direction is presented in Fig. 2. The deviations along the three reciprocal directions for all three Bragg reflections measured here clearly visualize both the domains and domain walls. For all three Bragg reflections, rather continuous variations of $\Delta\mu_x$ along the y-direction (horizontal) and $\Delta\mu_y$ along the x-direction (vertical) are visible signifying a tilting of the lattice planes. The domain walls are apparent by the discontinuous variation of $\Delta\mu_x$ and $\Delta\mu_y$ of the order of 1 x 10^{-1} Å^{-1} and 5 x 10^{-1} Å^{-1}, respectively, indicating a clear lattice distortion by these boundaries. For all three studied Bragg reflections the central domain exhibits a tensile strain ($\Delta\mu_z < 0$) with respect to the left and right domains and the domain walls show a clear compressive strain ($\Delta\mu_z > 0$). In addition, a defect-like structure is visible in the central domain. This defect structure may be due to beam damage caused during the alignment process prior to the recording of the 3D-RSM. The fact that it is located at different positions for the three

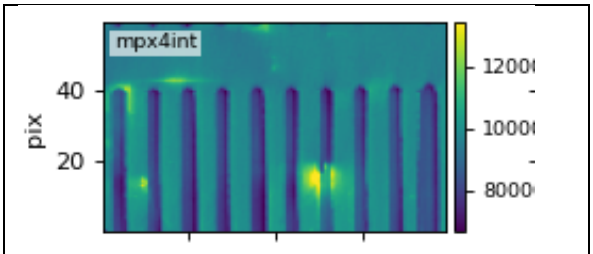

Fig. 1: Scanning X-ray diffraction map of a ppLN crystal taken at the (-2 4 -2 12) Bragg peak

investigated Bragg reflections may be caused by a projection effect due to different incident, respective, diffraction angles for the three different Bragg peaks.

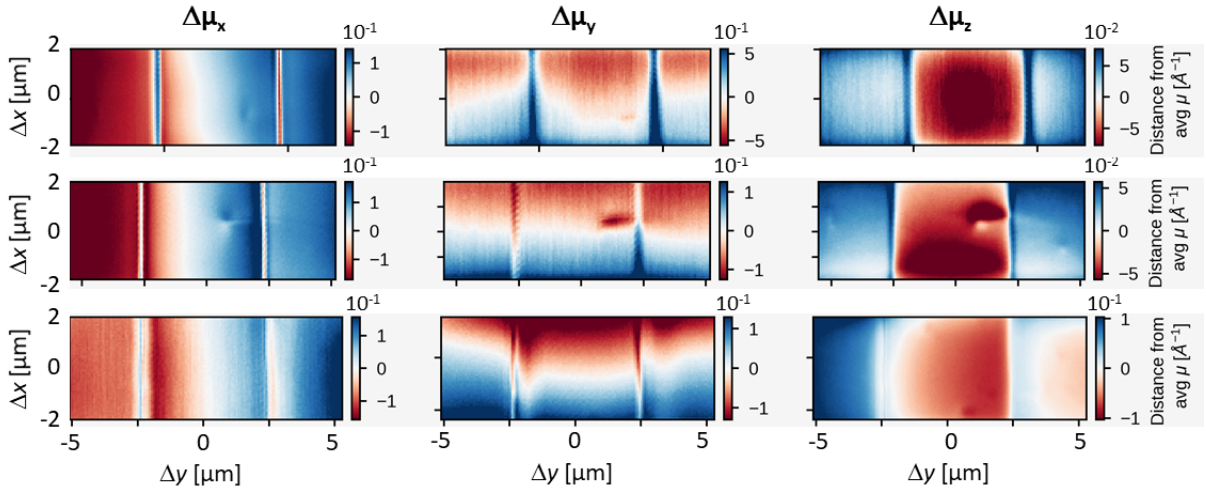

Fig. 2: Displacement of the Bragg reflection along the q_x, q_y and q_z direction for a) the 0 0 0 12, b) the 3 0 -3 12 and the c) -2 4 -2 12 $LiNbO_3$ Bragg peak.

Combining the measurements obtained for the three orthogonal Bragg reflections measured in this work, the six components ε_{11}, ε_{22}, ε_{33}, ε_{12}, ε_{13}, and ε_{23} of the strain tensor were inferred. The 2D strain maps for the six above mentioned strain components are presented in Fig. 3. The defect induced by the beam damage is clearly visible for the components ε_{11}, ε_{13}, and ε_{23}, while it does not generate any visible strain for the other three components. The diagonal components of the strain tensor vary in a range of about 2 x 10^{-5} whereas the three other components show a variation that is one to two orders of magnitude larger.

Linear profiles of the three diagonal components of the strain tensor along the dashed line indicated in the 2D maps (above the defect induced by the X-ray beam during alignment) are shown. The domain walls are clearly visible in the variation of all three strain tensor components. The ε_{11} strain increases by about 1 x 10^{-5} in the vicinity of the domain wall while ε_{33} decreases by about the same amount. The ε_{22}, on the contrary, diminishes for the left domain wall whereas it increases for the right one. For all three strain tensor components, the variation of the strain happens within +/- 200 nm in the vicinity of the domain walls. For the central domain and the two lateral domains, ε_{33} changes by about 1.5 x 10^{-5}.

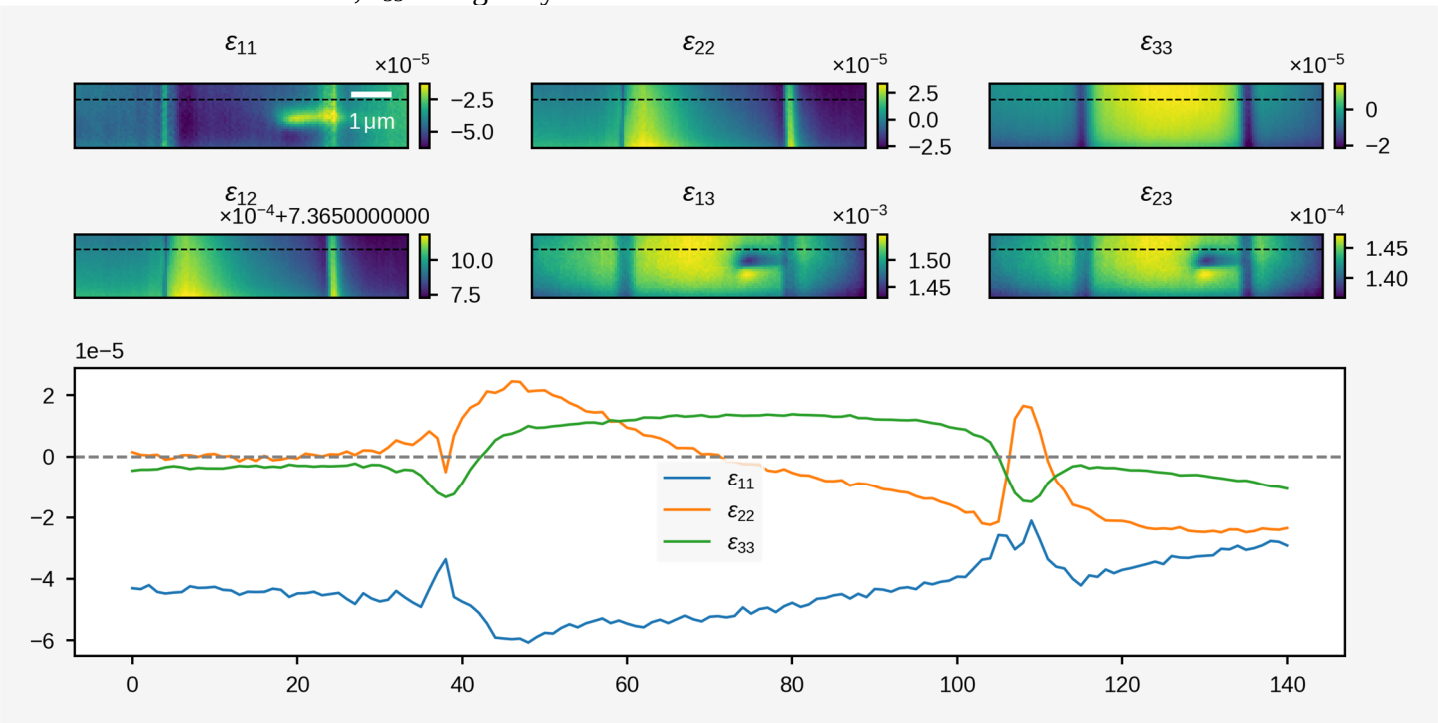

Fig. 3: 2D maps of the variation for 6 components of the strain tensor in ferroelectric domains in a periodically poled $LiNbO_3$ bulk crystal inferred from SXDM measured at three independent Bragg peaks. Linear profiles of the 3 diagonal components of the strain tensor.

Similar measurements were performed on an $ErMnO_3$ crystal. The SXDM of the non-polar surface of the crystal shows cloverleaf variations which are probably related to the domain structure in this crytal. The data on $ErMnO_3$ are still being analysed.

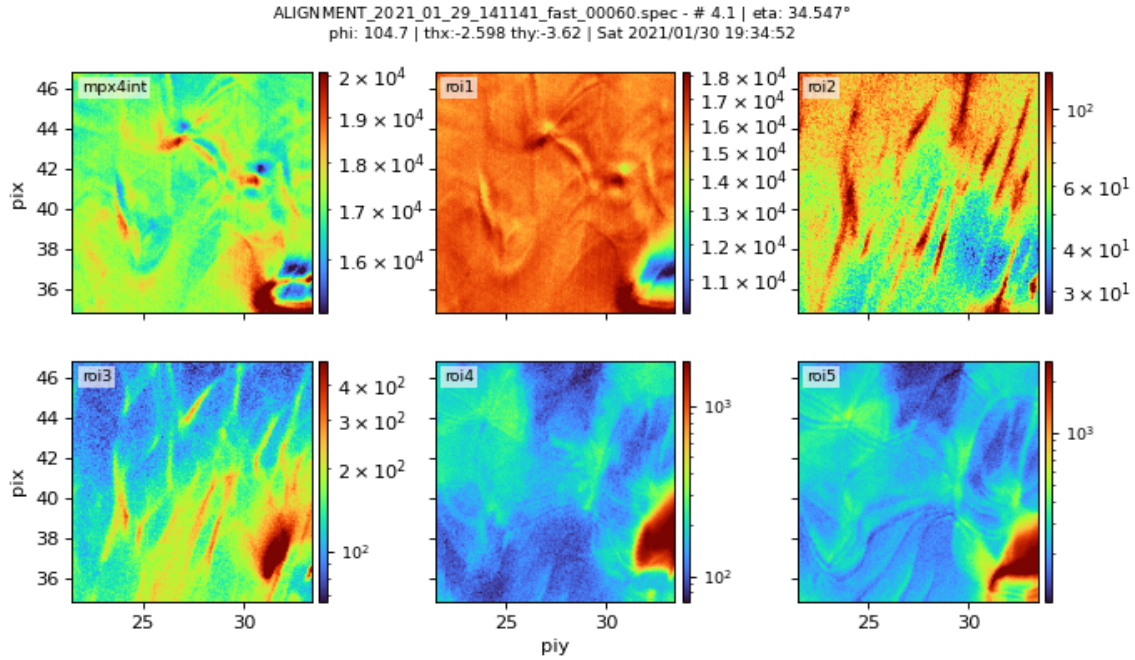

Fig. 4: Scanning X-ray diffraction map of the non-polar surface of a ErMnO3 crystal.

We demonsrtated successful SXDM of the ferroelectric domain structure in periodically poled $LiNbO_3$ and an $ErMnO_3$ crystal. These results pave the way for future studies on the ferroelectric domain structure in ferroelectric thin film using X-ray beams focused down to 25 nm.